Available online at www.sciencedirect.com
SCIENCE DIRECT®
Physica E 22 (2004) 365–368
PHYSICA E
www.elsevier.com/locate/physe

Quantum oscillation and decoherence in triangular antidot lattice

M. Ueki*, A. Endo, S. Katsumoto, Y. Iye

Institute for Solid State Physics, University of Tokyo, Kashiwa, Chiba 277-8581, Japan

Abstract

Quantum oscillation phenomena in triangular antidot lattice have been investigated. Altshuler–Aronov–Spivak oscillations and Aharonov–Bohm (AB)-type oscillations are observed at low magnetic field, and AB-type oscillations due to edge channels are observed in the quantum Hall regime. Measurements of the temperature dependence of these oscillations furnish information on the mechanism of decoherence in the antidot lattice, which is compared with the single ring case.

PACS: 73.23.Ad; 73.43.Qt

Keywords: Antidot lattice; AB-type oscillation; AAS oscillation; Decoherence

1. Introduction

Extensive studies have been carried out to elucidate electronic transport phenomena in two-dimensional electron gas (2DEG) at semiconductor heterointerface subjected to artificial potential modulations. Antidot lattices provide an experimental stage for interesting mixture of semiclassical and quantum transport phenomena. Quantum transport is manifested in Aharonov–Bohm (AB)-type oscillation [1,2] and Altshuler–Aronov–Spivak (AAS) oscillations [3]. Here, we study these effects in triangular antidot lattices with high regularity. We focus on the temperature dependence of the oscillation amplitude, i.e. decoherence at finite temperatures, for each type of quantum oscillatory phenomena in macroscopic antidot lattice, and make comparison with the cases of single quantum ring [4,5] and with the case of a mesoscopic system consisting of small number of antidots [6].

2. Experiment

Samples used in this work were fabricated from a GaAs/AlGaAs single heterojunction wafer with electron density $n_s = 3.6 \times 10^{15}$ m^{-2} and mobility $\mu = 68$ m^2/Vs. The corresponding Fermi energy was $E_F = 12$ meV and the elastic mean free path $\ell = 6.8$ μm. Triangular antidot lattice was fabricated on a standard Hall bar pattern by electron beam lithography and wet chemical etching, over the area 45×180 μm^2 between the voltage probes. Fig. 1 is a scanning electron micrograph of the triangular antidot lattice. The uniformity of the lithographical pattern is confirmed both by the micrograph and by observation of clear quantum oscillations which would be easily smeared by irregularity. The lattice constant was $a = 960$ nm and the geometrical aspect ratio was $d/a = 0.6$ (Sample #1)

* Corresponding author.
E-mail addresses: ueki@issp.u-tokyo.ac.jp (M. Ueki), iye@issp.u-tokyo.ac.jp (Y. Iye).

1386-9477/$ - see front matter
doi:10.1016/j.physe.2003.12.022

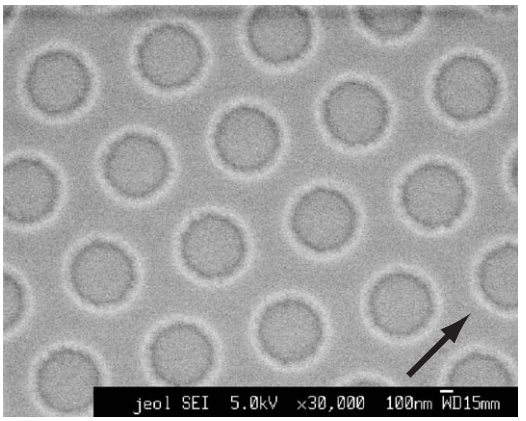

Fig. 1. Scanning electron micrograph image of triangular antidot lattice. The thick arrow indicates the current direction.

and 0.7 (Sample #2), d being the lithographical diameter of the antidot. With the depletion region around each antidot taken into account, the effective diameter is expected to be larger by ~ 100 nm.

Samples were cooled in a mixing chamber of a dilution refrigerator down to a base temperature of 30 mK. Magnetic field up to 15 T was applied parallel to the 2DEG plane by a superconducting solenoid. Resistance measurements were carried out by low frequency lock-in technique with a current bias typically set at 2 nA. The dependence on the bias current was checked at the lowest temperature.

3. Results and discussion

Fig. 2(a) shows the magnetoresistance of Sample #2 at 30 mK for the whole field range. The trace in the low field part is expanded in Fig. 2(b). The lower curve shows the oscillatory part of the magnetoresistance after subtracting the smooth background. The AAS ($h/2e$) oscillation around zero magnetic field and the AB-type (h/e) oscillation at somewhat higher fields are clearly identified. The periods of these oscillations are consistent with the unit cell area. The periodic orbit responsible for these two types of quantum oscillation is the one that encircles an antidot by bouncing from six neighboring antidots.

We have also observed quantum oscillations in the quantum Hall regime. Fig. 2(c) shows an expanded view of the trace near the peak at $B = 4.85$ T corresponding to the filling $\nu \approx 2.5$, transition region

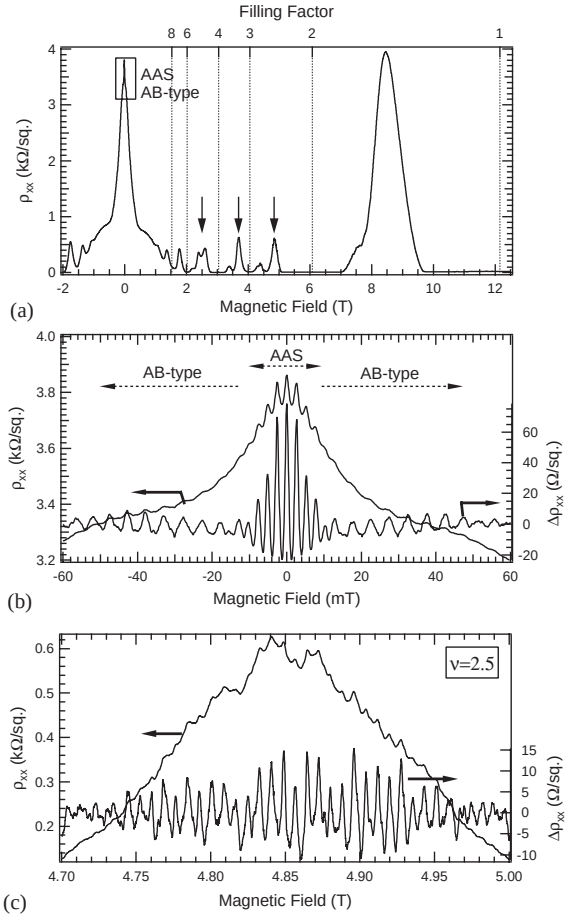

Fig. 2. (a) Magnetoresistance trace of Sample #2 at 30 mK. (b) An expanded view of the low field data. The lower curve is the oscillatory part obtained by subtracting the background negative magnetoresistance. AAS ($h/2e$) and AB-type (h/e) oscillations are clearly identified. (c) An expanded view around filling $\nu = 2.5$. The lower curve is the oscillatory part. AB-type oscillation with period longer than the low-field counterpart is observed.

between $\nu = 3$ and $\nu = 2$. Clear AB-type (h/e) oscillations are superposed on the background. Similar oscillatory behavior has been also seen for other peaks marked by arrows in Fig. 2(a). The period of the high-field oscillation is consistent with the area of the antidot with appropriate allowance for the depletion region, suggesting that these oscillations arise from the edge channel circumnavigating the antidot. The oscillation period increases systematically for higher filling factors (lower magnetic fields) reflecting the shift in the position of the outermost edge channel.

The observability of the quantum oscillations in antidot lattice depends on the symmetry of the lattice and the magnetic field range. The AAS oscillation is conspicuous in triangular lattice but absent in square lattice as shown by Nihey [3]. The AB-type oscillation is seen both in square and triangular lattices, and is prominent in the field range where the commensurability condition $2R_c \approx a$ (R_c: cyclotron radius) is satisfied [1–3].

The physical origin of the AAS oscillation in antidot lattice is basically the same as that in a single ring. Since the AAS oscillation originates from interference between states in time reversal symmetry, it is immune to the ensemble averaging, so that it can be observed in a macroscopic antidot lattice as long as the relevant ring area is uniform over the sample. By contrast, the phase of AB interference in a single ring is specific to the ring, so that ensemble averaging leads to destruction of the AB oscillation. In this sense the h/e oscillation observed in macroscopic antidot lattice is different in nature from the AB oscillation in single ring, hence the name "AB-type". The AB-type oscillation in antidot lattice is attributed to the oscillatory fine structure in the density of states spectrum such as calculated by Gutzwiller trace formula [1]. Full quantum mechanical calculations confirm this picture [8,9]. However, the subtle question how it is reflected in the conductivity is not fully answered [9].

The AB-type oscillation in the quantum Hall regime has been observed in a mesoscopic system consisting of small number of antidots [6], in which phase coherence is thought to be developed over the whole system. The present system is in a different regime in that the size of the antidot lattice is macroscopic and is much larger than the phase coherence length estimated to be on the order of a few μm at the lowest temperature.

We have investigated the temperature dependences of the three types of quantum oscillation. Fig. 3 shows the temperature dependences of the AAS oscillation amplitude in Samples #1 and #2. The amplitude of the fundamental period ($h/2e$) is shown together with those of the higher harmonics. The relative amplitude of the $h/2e$, $h/4e$ and $h/6e$ components are consistent with the expected dependence $\propto \exp(-nL/L_\phi)$, where L is the circumference of the antidot and n is the harmonic index. The phase coherence length is written as $L_\phi = v_F\tau_\phi$ for a ballistic system, where τ_ϕ is the phase relaxation time. With the temperature dependence of the phase coherence length written as $L_\phi \propto T^{-\alpha}$, the temperature dependence of the

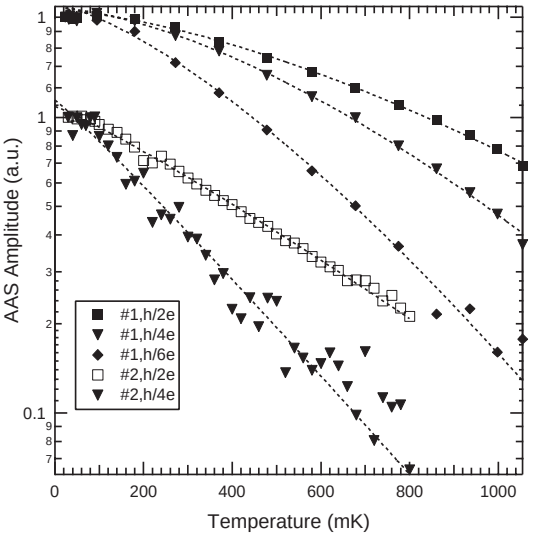

Fig. 3. The temperature dependence of the AAS oscillation amplitude for the two samples. In addition to the fundamental period ($h/2e$) component, the higher harmonic components ($h/4e$ and $h/6e$) are also shown.

AAS amplitude can be fitted to $\propto \exp\{-(T/T_c)^\alpha\}$. The best fit gives $\alpha = 1.49 \pm 0.05$ for Sample #1, which implies $L_\phi \propto T^{-1.5}$. For Sample #2, the value is $\alpha = 1.12 \pm 0.03$, i.e. the temperature dependence is closer to $L_\phi \propto T^{-1}$.

The electron–electron inelastic scattering time in a clean 2D system is given by $\tau_{e-e} \propto T^{-2} \ln T$. Different temperature dependences are predicted for disordered systems and lower dimensional systems [7]. For a dirty 2D system $\tau_{e-e} \propto T^{-1} \ln T$. At low temperatures, electron dephasing can be governed by Nyquist dephasing process, i.e. multiple small energy transfer scattering events, so that the phase relaxation time τ_ϕ can be quite different from the inelastic scattering time τ_{e-e}. The Nyquist dephasing time is given by $\tau_\phi \propto T^{-1}$ for dirty 2D and $\propto T^{-2/3}$ for dirty 1D system. For clean (ballistic) 2D systems, $\tau_\phi \propto T^{-2}$ is expected. On the other hand, $L_\phi \propto T^{-1}$ is generally observed for single AB rings with small number of conducting channels (1D case) [4,5]. The temperature dependence of L_ϕ found in Samples #1 and #2 are intermediate between these behaviors. It is interesting that the Sample #2, which has a larger aspect ratio and hence narrower channel, shows a dependence closer to $\propto T^{-1}$.

Fig. 4 shows the temperature dependence of the amplitude of the low-field AB-type oscillation and the

high field one at $\nu \approx 2.5$, respectively. They both obey $\propto \exp(-T/T^*)$. The relative magnitude of the harmonic component does not follow the kind of scaling seen in the case of AAS oscillation.

The characteristic temperature governing the decay of low-field AB-type oscillation was found to be $T^* = 0.69$ K for Sample #1 and 0.36 K for Sample #2. These values are of the order of the calculated energy level spacing of quantized orbits circumnavigating the antidot. However, there are a few points that cannot be readily explained from such level spacing argument. One is the difference of T^* by a factor of 2 between the two samples. Another is the behavior at low temperatures. The simple picture based on the oscillatory structures in the density of state spectrum predicts a temperature dependence of the form $x/\sinh(x)$ ($x = 2\pi^2 k_B T/\Delta E$ with ΔE the characteristic level spacing. The oscillation amplitude then should saturate at temperatures much lower than the scale of ΔE, in disparity with the observed exponential temperature dependence. This seems to indicate that it is insufficient to treat the problem only in terms of density of states spectrum. The precise role of phase coherence in the AB-type oscillation in macroscopic antidot system is not clear at the moment. This is an issue to be elucidated further.

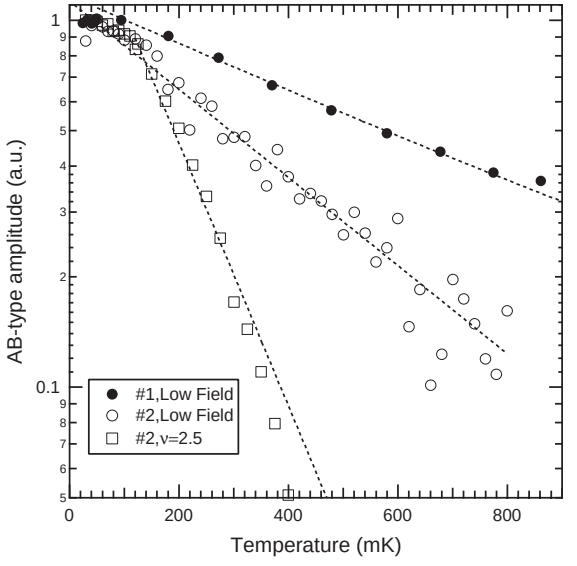

Fig. 4. The temperature dependence of the amplitude of the AB-type oscillations in the low region and that in the quantum Hall regime near $\nu = 2.5$.

The AB-type oscillation in the high field region turned out to be much more temperature sensitive. The temperature dependence is well fitted to the functional form $\propto \exp(-T/T^*)$. The characteristic temperature for the high field AB-type oscillation is found to be considerably lower than that for the low field AB-type oscillation. $T^* \simeq 0.12$ K for the oscillations around $\nu = 2.5$. Again, the difference in the value of T^* from those for the low field range cannot be readily explained by the level spacing argument.

4. Conclusion

We have observed three types of quantum oscillations in triangular antidot lattice systems. The temperature dependence of the AAS oscillation is given by $\propto \exp(-nL/L_\phi)$ with $L_\phi \propto T^\alpha$, α being ~ 1.5 and ~ 1.1 for the samples with aspect ratio 0.6 and 0.7, respectively. The AB-type oscillations in the low- and high field regions both obey the exponential temperature dependence $\propto \exp(T/T^*)$. The value of the characteristic temperature T^* is smaller for the high field AB-type oscillation. The oscillation amplitude follows an exponential temperature dependence which cannot be readily explained within the simple picture of the oscillatory structure in the density of state spectrum.

Acknowledgements

The work is supported in part by Grant-in-Aid for Scientific Research from the Ministry of Education, Culture, Sport, Science and Technology (MEXT), Japan.

References

[1] D. Weiss, K. Richiter, A. Menschig, R. Bergmann, H Schweizer, K. von Klitzing, Phys. Rev. Lett. 70 (1993) 4118.
[2] F. Nihey, K. Nakamura, Physica B 184 (1993) 398.
[3] F. Nihey, S.W. Hwang, K. Nakamura, Phys. Rev. B 51 (1995) 4649.
[4] A.E. Hansen, A. Kristensen, S. Pedersen, C.B. Sørensen, P.E. Lindelof, Phys. Rev. B 64 (2001) 045327.
[5] K. Kobayashi, H. Aikawa, S. Katsumoto, Y. Iye, J. Phys. Soc. Japan 71 (2002) 2094.
[6] R. Schuster, K. Ensslin, V. Dolgopolov, J.P. Kotthaus, G. Bohm, W. Klein, Phys. Rev. B 52 (1995) 14699.
[7] J.J. Lin, J.P. Bird, J. Phys.: Condens. Matter 14 (2002) R501.
[8] H. Silberbauer, U. Rossler, Phys. Rev. B 50 (1994) 11911.
[9] S. Ishizaka, F. Nihey, K. Nakamura, J. Sone, T. Ando, Phys. Rev. B 51 (1995) 9881;
S. Uryu, T. Ando, Phys. Rev. B 53 (1996) 13613.